HHS Public Access

Author manuscript

Free Radic Biol Med. Author manuscript; available in PMC 2016 December 01.

Published in final edited form as:

Free Radic Biol Med. 2015 December ; 89: 690–700. doi:10.1016/j.freeradbiomed.2015.08.028.

Systemic administration of the apocarotenoid bixin protects skin against solar UV-induced damage through activation of NRF2

Shasha Tao[1], **Sophia L. Park**[1], **Montserrat Rojo de la Vega**[1], **Donna D. Zhang**[1,*], and **Georg T. Wondrak**[1,*]

[1]Department of Pharmacology and Toxicology, College of Pharmacy & Arizona Cancer Center, University of Arizona, Tucson, AZ, USA

Abstract

Exposure to solar ultraviolet (UV) radiation is a causative factor in skin photodamage and carcinogenesis, and an urgent need exists for improved molecular photoprotective strategies different from (or synergistic with) photon absorption. Recent studies suggest a photoprotective role of cutaneous gene expression orchestrated by the transcription factor NRF2 (nuclear factor-E2-related factor 2). Here we have explored the molecular mechanism underlying carotenoid-based systemic skin photoprotection in SKH-1 mice and provide genetic evidence that photoprotection achieved by the FDA-approved apocarotenoid and food additive bixin depends on NRF2 activation. Bixin activates NRF2 through the critical Cys-151 sensor residue in KEAP1, orchestrating a broad cytoprotective response in cultured human keratinocytes as revealed by antioxidant gene expression array analysis. Following dose optimization studies for cutaneous NRF2 activation by systemic administration of bixin, feasibility of bixin-based suppression of acute cutaneous photodamage from solar UV exposure was investigated in *Nrf2*$^{+/+}$ versus *Nrf2*$^{-/-}$ SKH-1 mice. Systemic administration of bixin suppressed skin photodamage, attenuating epidermal oxidative DNA damage and inflammatory responses in *Nrf2*$^{+/+}$ but not in *Nrf2*$^{-/-}$ mice, confirming the NRF2-dependence of bixin-based cytoprotection. Taken together, these data demonstrate feasibility of achieving NRF2-dependent cutaneous photoprotection by systemic administration of the apocarotenoid bixin, a natural food additive consumed worldwide.

Abstract

[*]**Corresponding authors:** Georg T. Wondrak, wondrak@pharmacy.arizona.edu, Phone: 520-626-9009, Fax: 520-626-379, Donna D. Zhang, dzhang@pharmacy.arizona.edu, Phone: 520-626-9918, Fax: 520-626-2466.

CONFLICT OF INTEREST

The authors state no conflict of interest.

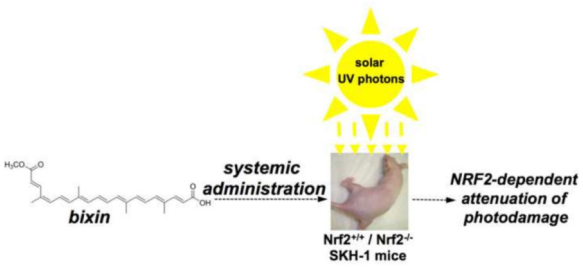

Keywords

bixin; skin photodamage; NRF2; antioxidant gene expression; systemic photoprotection

INTRODUCTION

Exposure to solar ultraviolet (UV) radiation is a causative factor in skin photodamage and carcinogenesis [1-3]. Even though sunscreen-based broad-spectrum photoprotection is an effective key component of a sun-safe strategy to reduce cumulative lifetime exposure to UV light, much effort has been directed towards the development of more effective molecular strategies for cutaneous photoprotectants acting through mechanisms different from (or synergistic with) photon absorption [4-7].

The redox-sensitive transcription factor NRF2 (nuclear factor-E2-related factor 2) orchestrates major cellular defense mechanisms including phase-II detoxification, inflammatory signaling, DNA repair, and antioxidant response, and NRF2 has therefore emerged as a promising molecular target for the pharmacological prevention of human pathologies resulting from exposure to environmental toxicants including solar UV light [8-11]. Recent studies strongly suggest a protective role of NRF2-mediated gene expression in the suppression of cutaneous photodamage induced by solar UV radiation, and NRF2 activation has been shown to protect cutaneous keratinocytes and fibroblasts against the cytotoxic effects of UVA and UVB [9, 11-21]. Importantly, recent research performed in SKH-1 mice documents that constitutive genetic NRF2 activation protects mice against acute photodamage and photocarcinogenesis [22]. Therefore, pharmacological modulation of NRF2 has now attracted considerable attention as a novel approach to skin photoprotection [19, 21, 23]. Indeed, protection of primary human keratinocytes from UVB-induced cell death by novel drug-like NRF2 activators has been reported, a photoprotective effect attributed in part to NRF2-dependent elevation of cellular glutathione levels [20, 24, 25]. Topical application of NRF2 inducers, e.g. the synthetic NRF2-activator TBE-31, has shown pronounced photoprotective and photochemopreventive activity in murine skin, and suppression of solar UV-induced human skin erythema was achieved by topical application of a standardized broccoli extract delivering the NRF2 inducer sulforaphane [22]; however, there has been little research exploring the concept of cutaneous photoprotection and photochemoprevention achieved by systemic administration of NRF2 inducers [26].

Dietary carotenoids (including β-carotene, lycopene, lutein, 3,3'-dihydroxyisorenieratene, zeaxanthin, astaxanthin) and their biosynthetic precursor molecules (such as phytoene) have

been under investigation for cutaneous photoprotection, and feasibility of carotenoid-based nutritional photoprotection has been demonstrated in murine and human skin [4, 27-30]. The systemic photoprotective activity of carotenoids, displayed only after dietary uptake and cutaneous accumulation, has largely been attributed to their activity as photon absorbers, sacrificial antioxidants, and excited state/singlet oxygen quenchers [30-32]. However, the mechanistic involvement of NRF2 activation in carotenoid-based systemic photoprotection has not been investigated before.

In an attempt to test the feasibility of NRF2-dependent systemic photoprotection by dietary constituents, we focused our photoprotection studies on the apocarotenoid bixin, an FDA-approved natural food colorant from the seeds of the achiote tree (*Bixa orellana*) native to tropical America [33, 34]. Consumed by humans since pre-Columbian times, this apocarotenoid derived from lycopene through oxidative cleavage is now used worldwide as a dietary additive and cosmetic ingredient (referred to as 'annato'; E160b) with an excellent safety record and established systemic bioavailability and pharmacokinetic profile upon oral administration [35-37]. Here, we report for the first time that (*i*) bixin is a potent activator of the NRF2-dependent cytoprotective response in cultured human skin keratinocytes, that (*ii*) systemic administration of bixin activates cutaneous NRF2 with potent protective effects against solar UV-induced skin damage in SKH-1 mice, and that (*iii*) bixin-induced suppression of photodamage is observable in $Nrf2^{+/+}$ but not in $Nrf2^{-/-}$ SKH-1 mice confirming the NRF2-dependence of bixin-based antioxidant and anti-inflammatory cutaneous effects.

MATERIALS AND METHODS

Chemicals, antibodies, and cell culture

Bixin was purchased from Spectrum (New Brunswick, NJ); sodium arsenite (As), cycloheximide, and MG132 were from Sigma (St. Louis, MO); sulforaphane (SF) was purchased from Santa Cruz (Santa Cruz, CA); primary antibodies against NRF2, KEAP1, GCLM, AKR1C1, NQO1, AKR1C2, HO-1, TrxR, FTH (heavy), MMP9, Ki67, and GAPDH, as well as horseradish peroxidase (HRP)-conjugated secondary antibodies were purchased from Santa Cruz. Antibodies against p-P65 and P65 were purchased from Cell Signaling. The anti-Thymine Dimer (H3) CPD antibody was purchased from Novus (Littleton, CO). The hemagglutinin (HA) epitope antibody was purchased from Covance (Branford, CT). The 8-oxo-dG antibody was purchased from Trevigen (Gaithersburg, MD). Human immortalized HaCaT keratinocytes were grown in Dulbecco's Modified Eagle Medium (DMEM) supplemented with 10% fetal bovine serum and 0.1% gentamycin, and primary human epidermal keratinocytes [adult HEKa (C-005-5C)] were cultured on collagen matrix protein-coated dishes using Epilife medium (EDGS growth supplement; Life Technologies, Carlsbad, CA).

Irradiation with solar UV light

Irradiation with solar UV occurred as described before [38-40]. A KW large area light source solar simulator, model 91293, from Oriel Corporation (Stratford, CT) was used, equipped with a 1000 W Xenon arc lamp power supply, model 68920, and a VIS-IR

bandpass blocking filter combined with an atmospheric attenuation filter (output 290-400 nm plus residual 650-800 nm). At 345 mm from the source, the UV dose was 4.4 J/cm^2 UVA + 240 mJ/cm^2 UVB radiation.

Bixin mass spectrometry and detection in mouse plasma

Electrospray mass spectrometry of bixin [dissolved in tetrahydrofuran and diluted tenfold in acetonitrile/NH_4OH (0.1 N); ESI-MS (negative ion mode) m/z 393.21 $(M-1)^-$] was performed using a Bruker Apex FT/ICR mass spectrometer. For determination of bixin plasma levels, mouse samples were subjected to chloroform extraction followed by analysis using a Thermo Finnigan Surveyor HPLC system with photodiode array detector (300-580 nm) using a Luna RP-C18 column (3 μ; 100 × 4.6 mm; Phenomenex, Torrance, CA) with mobile phase A (water, 0.1 % formic acid) and mobile phase B (acetonitrile, 0.1 % formic acid); gradient: 0 min: 20% A; 10 min: 5% A; 15 min 0% A.

Human Oxidative Stress RT^{2}Profiler™ PCR Expression array analysis

Total cellular RNA was prepared according to a standard procedure using the RNeasy kit (Qiagen, Valencia, CA, USA). Reverse transcription was performed using the RT^2 First Strand kit (SuperArray, Frederick, MD, USA) and 1 μg total RNA. The Human Oxidative Stress RT^{2}Profiler™ PCR Expression Array (SuperArray) profiling the expression of 84 stress-related genes was employed as described before [41, 42]. Gene-specific product was normalized to *ACTB* and quantified using the comparative ($\Delta\Delta C_t$) Ct method following the ABI Prism 7000 sequence detection system user guide. Expression values were averaged across three independent array experiments followed by statistical analysis.

Cell viability

Bixin cytotoxicity was assessed by flow cytometric analysis of annexinV/PI-stained cells using a commercial kit from Sigma (APO-AF, St. Louis, MO) as published before [40,42]. Bixin toxicity was also assessed examining functional impairment of mitochondria using the 3-(4,5-dimethylthiazol-2-yl)-2,5-diphenyltetrazolium bromide (MTT) standard assay [43]. Approximately 1 × 10^4 HaCaT cells were seeded in a 96-well plate, and 24 h later the cells were treated with the indicated doses of bixin for another 48 h. After treatment, 20 μL of 2 mg/mL MTT were directly added to the cells, followed by incubation at 37 °C for 2 h. 100 μl of isopropanol/HCl were added to each well and the plate was shaken at room temperature to dissolve the crystals. Absorbance was measured at 570 nm using the Synergy 2 Multi-Mode Microplate Reader (Biotek).

Glutathione assay

Total intracellular glutathione in cultured cells was analyzed using the luminescent GSH-Glo glutathione assay (Promega). Cells were harvested and then counted using a Z2 Coulter counter, and GSH was determined per 10,000 viable cells. Data represent relative levels of glutathione normalized for cell number (treated versus solvent controls).

Detection of intracellular oxidative stress by flow cytometric analysis

Photodynamic induction of intracellular oxidative stress and its suppression by bixin pretreatment was analyzed by flow cytometry using 2',7'-dichlorodihydrofluorescein diacetate (DCFH-DA) as a sensitive non-fluorescent precursor dye according to a published standard procedure [14]. HaCaT keratinocytes were pretreated with bixin (1 or 24 h) and then exposed to singlet oxygen generated by dye-sensitization as described earlier [14, 44]. In brief, toluidine blue O (TB) photosensitization was achieved using a 'Sylvania 15 W Cool White' light tube delivering visible light at an irradiance of 4.29 mW/cm^2. The irradiance in the visible region (400-700 nm) was determined using a spectroradiometer, Model 754 from Optronic Laboratories (Orlando, FL). Cells received visible radiation at a distance of 50 mm from the source through the polystyrene lids of cell culture dishes. For $^1O_2$ exposure, cells were washed with PBS and immediately exposed to the combined action of visible light (0.3 J/cm^2) and TB (3.3 μM) in PBS. Following 5 min incubation in the dark after irradiation, cells were washed with PBS. Cells were then incubated for 60 min in the dark (37 °C, 5% CO_2) with culture medium containing DCFH-DA (5 μg/mL final concentration). Cells were then washed with PBS, harvested by trypsinization, resuspended in 300 μ l PBS, and analyzed by flow cytometry.

Transfection of cDNA and luciferase reporter gene assay

Transfection of cDNA was performed using Lipofectamine 3000 (Invitrogen) according to the manufacturer's instructions. Activation of NRF2 transcriptional activity was performed as previously published [14, 43]. Briefly, HaCaT cells were cotransfected with expression vectors for either *KEAP1* wild type (*KEAP1-WT*) or *KEAP1* with a mutation that generates a protein that contains a serine residue instead of a cysteine (*KEAP1-C151S*), along with *NQO1-ARE* firefly luciferase and *Renilla* luciferase reporters. At 24 h post-transfection, cells were left untreated or treated with SF (5 μM), As (5 μM), or bixin (40 μM) for 16 h. The cells were then lysed for analysis of the reporter gene activity using the Promega dual-luciferase reporter gene assay system.

Immunoblot analysis, ubiquitylation assay, and protein half-life

Experiments were performed according to previously published procedures [43]. Cells were harvested in sample buffer (50 mM Tris-HCl [pH 6.8], 2% sodium dodecyl sulfate (SDS), 10% glycerol, 100 mM dithiothreitol (DTT), and 0.1% bromophenol blue), boiled and sonicated. Total cell lysates were resolved by SDS-PAGE and subjected to immunoblot analyses with the indicated antibodies. For the ubiquitination assay, cells were cotransfected with expression vectors for *NRF2* and HA-tagged ubiquitin (*HA-Ub*). Cells were left untreated or treated with either 5 μM sulforaphane (SF) or 40 μM bixin along with 10 μM MG132 for 4 h. Cells were harvested in buffer containing 2% SDS, 150 mM NaCl, 10 mM Tris-HCl (pH 8.0), and 1 mM DTT and boiled immediately. For immunoprecipitation, 1 μg of NRF2 antibody was incubated with the cell lysates at 4°C overnight with protein A agarose beads (Invitrogen). Immunoprecipitated complexes were washed four times with RIPA buffer and eluted in sample buffer by boiling for 5 min. Samples were resolved by SDS-PAGE and immunoblotted with HA antibody. To measure the half-life of NRF2, HaCaT cells were either left untreated or treated with 5 μM bixin for 4 h, then 50 μM

cycloheximide was added to block protein synthesis. Total cell lysates were collected at different time points and subjected to immunoblot analysis with NRF2 antibody. The relative intensity of the bands was quantified using the ChemiDoc CRS gel documentation system and Quantity One software (BioRad).

mRNA extraction and real-time RT-PCR

Total RNA was extracted from HaCaT cells and mouse skin tissues using TRIzol (Invitrogen). Equal amounts of mRNA were used to generate cDNA using the M-MLV Reverse Transcriptase synthesis kit according to the manufacturer's instructions (Promega). RT-PCR and primer sequences of *NRF2*, *KEAP1*, *GCLM*, *AKR1C1* and *GAPDH* were described previously to evaluate mRNA expression using the LightCycler 480 system (Roche) [21, 43]. Quantification of cDNA amount for mouse *Nrf2*, *Keap1*, *Gclm*, and *Akr1c1* in each skin tissue sample was performed using the KAPA SYBR FAST qPCR Kit (Kapa Biosystems).

All primer sets were designed with Primer 3 online free software (http://www-genome.wi.mit.edu/genome_software/other/primer3.html) and were synthesized by Sigma as follows:

Nrf2: forward (CTCAGCATGATGGACTTGGA)

reverse (TCTTGCCTCCAAAGGATGTC);

Keap1: forward (GATCGGCTGCACTGAACTG)

reverse (GGCAGTGTGACAGGTTGAAG);

Akr1c1: forward (GGAGGCCATGGAGAAGTGTA)

reverse (GCACACAGGCTTGTACCTGA);

Gclm: forward (TCCCATGCAGTGGAGAAGAT)

reverse (AGCTGTGCAACTCCAAGGAC);

IL6: forward (CCGGAGAGGAGACTTCACAG)

reverse (TCCACGATTTCCCAGAGAAC);

*TNF*α: forward (AGCCCCCAGTCTGTATCCTT)

reverse (GGTCACTGTCCCAGCATCTT);

Mmp9: forward (CAATCCTTGCAATGTGGATG)

reverse (AGTAAGGAAGGGGCCCTGTA);

(β-*actin*: forward (AAGGCCAACCGTGAAAAGAT)

reverse (GTGGTACGACCAGAGGCATAC).

The RT-PCR conditions used were the following: one cycle of initial denaturation (95 °C for 3 min), 40 cycles of amplification (95 °C for 10 s, 60 °C for 20 s, and 72 °C for 5 s), melting curve (95 °C for 5 s, 65 °C for 1 min, and 97 °C continuous), and a cooling cycle (40 °C for 30 s). Mean crossing point (Cp) values and standard deviations (SD) were determined. Cp values were normalized to the respective Cp values of the mouse (J-*actin* reference gene. Data are presented as a fold change in gene expression compared to the control group.

Animals and treatments

Nrf2$^{+/+}$ and *Nrf2*$^{-/-}$ SKH-I mice were obtained by breeding *Nrf2* heterozygous mice generated by back-crossing *Nrf2*$^{-/-}$ C57BL/6 mice onto the SKH-1 hairless mouse genetic background for at least six generations (JAX® Mice, The Jackson Laboratory) [45]. All animals received water and food ad libitum and were handled according to the Guide for the Care and Use of Laboratory Animals; the protocols were approved by the University of Arizona Institutional Animal Care and Use Committee. Eight-week-old *Nrf2*$^{+/+}$ and *Nrf2*$^{-/-}$ mice were randomly allocated into four groups (n = 6): (*i*) control (corn oil); (*ii*) bixin (200 mg/kg, dissolved in corn oil); (*iii*) UV; (*iv*) bixin+UV. Bixin was administered through intraperitoneal (*i.p.*) injection 48 h before UV exposure.

Skin tissue collection, H&E staining, and IHC

24 h after UV exposure, the mice were euthanized and back skin was collected and divided into two parts: one part was frozen in liquid nitrogen for total RNA extraction and protein analysis; the other part was fixed in 10% buffered formalin and embedded in paraffin for histological and immunohistochemical analyses. Tissue sections (4 μm) were baked and deparaffinized. Hematoxylin and eosin (H&E) staining was performed for pathological examination. Antigen retrieval was carried out by boiling the slides with retrieval solution (citric acid monohydrate 2.1 g/L in H_2O pH=6.0) three times for 5 min [43]. Tissue sections were then exposed to 3.5 M HCl for 15 min at room temperature and washed with PBS. Subsequently, tissue sections were treated with 0.3% peroxidase to quench endogenous peroxidase activity. Tissue sections were incubated with 5% normal goat serum for 30 min followed by 2 h incubation with primary antibodies at 1:100 dilution at room temperature. Staining was performed using the EnVision+System-HRP (DAB) kit (Dako) according to the manufacturer's instructions.

In situ TUNEL assay

An *in situ* cell death detection kit (Roche) was used for detection of apoptotic cell death in skin sections according to the manufacturer's instructions. Briefly, tissue sections were pretreated with proteinase K (20 μg/ml) in 10 mM Tris/HCl (pH 7.8) at 37 °C for 30 min. After washing three times with PBS, tissue sections were incubated with TUNEL reaction mixture for 1 h at 37 °C in the dark. Tissue sections were then stained with Hoechst, and analyzed using a fluorescence microscope (Zeiss Observer.Zi microscope; slidebook computer program; excitation wavelength: 450-500 nm; detection wavelength: 515-565 nm). Hoechst stain was visualized under UV light.

Statistical analysis

Results are presented as the mean ± SD of at least three independent experiments performed in duplicate or triplicate each. Statistical tests were performed using SPSS 13.0. Unpaired Student's t-tests were used to compare the means of two groups, and selected data sets were analyzed employing one-way analysis of variance (ANOVA) with Tukey's post hoc test; differences between groups were considered significant at $p < 0.05$.

RESULTS

Bixin activates NRF2 and NRF2 target gene expression with upregulation of antioxidant defenses in human keratinocytes

First, to comprehensively monitor antioxidant response gene expression induced by bixin (20 μM, 24 h) in primary human epidermal keratinocytes (HEKs) Oxidative Stress RT^2 Profiler™ PCR Expression Array analysis was performed (Fig. 1A). Pronounced upregulation of established NRF2 target genes involved in antioxidant protection and redox homeostasis (including AKR1C2, GCLC, NQO1, SLC7A11, FTH1, TXNRD1, NCF2, SRXN). Immunoblot analysis confirmed NRF2 activation in HEKs in response to bixin treatment as evident from increased protein levels of NRF2 and NRF2 targets including NQO1, AKR1C2, HO-1, TrxR, GCLM, SRXN1, and FTH1 (Fig. 1B left: < 20 μM, 24 h; Fig. 1B right: exposure time < 24 h, bixin 20 μM).

Next, the molecular mechanism underlying NRF2 activation by bixin was investigated in immortalized human HaCaT keratinocytes. Employing a dual luciferase ARE-reporter assay, dose-dependent induction of NRF2 transcriptional activity was elicited by bixin treatment, observable at concentrations (10-40 μ M) devoid of cytotoxicity as detected employing the photometric MTT assay (Fig. S1A; Supplementary Material) and flow cytometric assessment of annexinV-PI stained cells (Fig. S1B; Supplementary Material). Time course analysis revealed a rapid induction of NRF2 protein levels detectable within 2 h treatment, while no changes in KEAP1 protein levels were observed (Fig. 1D). Moreover, NRF2 target proteins including GCLM and AKR1C1 (Fig. 1D and Fig. S1C; Supplementary Material) were upregulated in response to bixin treatment, and bixin-based upregulation of NRF2 was sustained over the course of the 24 h treatment, whereas upregulation of GCLM persisted over an extended period (48h; Fig. 1D). Consistent with upregulation of glutathione biosynthesis factors (GCLM), total cellular glutathione was increased by almost 50% in response to bixin exposure (Fig. 1E). Since it has already been established that bixin displays potent activity as a direct physical singlet oxygen ($^1O_2$) quencher [30-32], we examined if bixin pretreatment was able to protect HaCaT cells against $^1O_2$-induced photo-oxidative stress (Fig. 1F). Using flow cytometric detection of DCF fluorescence intensity [after $^1O_2$-exposed cells were loaded with 2',7'-dichlorodihydrofluorescein diacetate (DCFH-DA)], it was observed that bixin (20 μM) pretreatment efficiently suppressed the almost five fold increase in DCF fluorescence elicited by $^1O_2$ originating from dye sensitization (employing an established toluidine blue/visible light-based regimen) [14, 44]. Remarkably, only prolonged preincubation (24 h) with bixin (20 μM) protected HaCaT cells against oxidative stress originating from dye sensitization. In contrast, shorter preincubation periods (1 h) were without protective effects, an observation consistent with the mechanistic

involvement of bixin-induced upregulation of cellular antioxidant defenses underlying cytoprotective effects against photooxidative stress. However, the extent of bixin-induced cytoprotection did not reach the level of cytoprotective efficacy displayed by the physical $^1O_2$-quencher NaN_3 (10 mM), active only if present during visible light-driven dye sensitization (Fig. 1F). We also observed that exposure to bixin only (1 or 24 h exposure time) did not cause an increase in DCF fluorescence (Fig. 1F). Moreover, bixin-induced upregulation of Nrf2 protein levels was not attenuated by cotreatment with various anti-oxidants [tiron, trolox, N-acetyl-L-cysteine (NAC); Fig. 1G][46]. Likewise, 24 h preincubation using NAC did not attenuate bixin-induced Nrf2 upregulation (data not shown), indicating that bixin does not cause Nrf2 upregulation through induction of intracellular oxidative stress.

Bixin activates NRF2 in a KEAP1-C151 dependent manner and increases Nrf2 protein half-life ($t_{1/2}$) in human keratinocytes

As indicated already by expression array analysis (Fig. 1A), it was also observed that bixin treatment caused pronounced upregulation of NRF2 target genes at the mRNA level without affecting *NRF2* or *KEAP1* mRNA levels (Fig. 2A-D), suggesting that bixin-based NRF2 activation occurs at the posttranscriptional level [43].

Next, the effect of bixin treatment on the half-life ($t_{1/2}$) of endogenous NRF2 protein was determined. Cycloheximide was added to untreated or bixin-treated cells to block *de novo* protein synthesis, and cells were harvested at different time points followed by immunoblot analysis (Fig. 2E, upper panel), and intensity of the NRF2 band was quantified to calculate NRF2 half-life (Fig. 2E, bottom panel). It was observed that $t_{1/2}$ of NRF2 of untreated cells was 20.5 min; however, after bixin treatment $t_{1/2}$ of NRF2 increased to 30.6 min.

In order to test if bixin-based NRF2 activation occurs through inhibition of KEAP1-mediated ubiquitination, a cell-based ubiquitination assay was performed in HaCaT cells cotransfected with expression vectors for *NRF2* and HA-tagged ubiquitin (*HA-Ub*) (Fig. 2F) [43]. To this end, cells were either exposed to bixin (40 μM) or sulforaphane (SF; 5 μM, positive control) or left untreated, combined with proteasome inhibition (MG132; 10 μM, 4 h). In response to bixin exposure, a dramatic reduction of NRF2-ubiquitination compared to the untreated control occurred, a response similar to the established inhibitory effects of SF on NRF2-ubquitination.

Since it has been shown previously that NRF2 activation by canonical inducers (including SF and tBHQ) depends on C (Cys)-151, a critical cysteine residue in KEAP1, we examined the mechanistic involvement of KEAP1-C151 bixin-based NRF2 activation [47, 48]. HaCaT cells were cotransfected with expression vectors for either KEAP1 wild type (*KEAP1-WT*) or a mutant KEAP1 (*KEAP1-C151S;* Cys-151 mutated to serine) along with *ARE*-firefly luciferase and *Renilla* luciferase reporters to assess NRF2 transcriptional activity (Fig. 2G). After exposure to SF (5 μM), As (sodium arsenite; 5 μM), or bixin (40 μM; all 16 h), NRF2 transcriptional activity was enhanced by all treatments in *KEAP1-WT* cells, whereas NRF2 activation by SF or bixin was abolished in *KEAP1-C151S* cells. In contrast, As treatment was equally effective causing NRF2 transcriptional activation in the *KEAP1-C151S* cells, an observation consistent with our previous report that this compound is a non-canonical NRF2

inducer that operates through a KEAP1-C151-independent mechanism [47, 48]. Taken together, these results demonstrate that bixin is a canonical NRF2 inducer acting through the critical Cys-151 sensor residue in KEAP1.

Systemic administration of bixin activates cutaneous NRF2 and suppresses UV-induced skin photodamage in $Nrf2^{+/+}$ but not $Nrf2^{-/-}$ mice

To explore the potential systemic photoprotective activity of bixin in a murine skin sunburn model, we first examined feasibility of upregulating cutaneous NRF2 activity by systemic administration. It has been reported earlier that efficient cutaneous accumulation of dietary carotenoids requires prolonged nutritional supplementation over weeks and that pharmacokinetic parameters of cutaneous delivery of dietary carotinoids differ between humans and mice [30]. Therefore, in order to circumvent the more complex pharmacokinetics associated with dietary supplementation, we chose an intraperitoneal (i.p.) route for bixin systemic administration followed by examination of cutaneous NRF2 status. After i.p. injection of bixin (200 mg/kg) performed in *Nrf2*$^{+/+}$ and *Nrf2*$^{-/-}$ mice, plasma was collected at 0, 1, 2, 4, 8, 16, 24, 48 and 72 h after injection followed by HPLC-photodiode array detection (Fig. S2A-C; Supplementary Material). Bixin peak plasma concentrations (C_{max}; up to 11.3 μg/ml) were reached at 2 h post injection before returning to basal levels at about 48 h, and AUC ('area under the curve' equaling total drug exposure) did not differ significantly between genotypes (Fig. S2C; Supplementary Material). Next, efficacy of various bixin treatment regimens (differing with regard to total dose and time after injection) for maximum activation of the NRF2 pathway in murine skin was determined (Fig. S2D; Supplementary Material). It was observed that administration of bixin (200 mg/kg, 72 h after injection) was most effective in upregulating cutaneous protein levels of NRF2 and its targets (GCLM and AKR1C1) in *Nrf2*$^{+/+}$ mice.

Next, the feasibility of bixin-induced cutaneous protection was studied in a solar UV photodamage model. *Nrf2*$^{+/+}$ and *Nrf2*$^{-/-}$ mice were i.p. injected with either corn oil (carrier control) or bixin (200 mg/kg) 48 h before solar UV exposure (240 mJ/cm^2 UVB; 4.4 J/cm^2 UVA) [39]. 24 h after UV exposure back skin tissue was then collected followed by immunohistochemical (IHC) analysis. As expected, bixin treatment dramatically induced the cutaneous NRF2 pathway in *Nrf2*$^{+/+}$ but not in *Nrf2*$^{-/-}$ mice, detectable at the protein [NRF2, GCLM, AKR1C1 (Fig. 3A-B) and mRNA levels (Fig. 3C-D). The mRNA levels of *Nrf2* did not increase in the bixin treatment groups, and bixin had no effects on protein or mRNA levels of *Keap1* (Fig. 3B and Fig. S3; Supplementary Material). Moreover, UV exposure alone activated the NRF2 response in murine skin, effects not detectable in *Nrf2*$^{-/-}$ mice (Fig. 3).

Remarkably, UV exposure caused a pronounced increase in epidermal thickness (Fig. 4A-B), accompanied by the detection of apoptotic (TUNEL-positive) cells located in the basal layer of the epidermis (Fig. 4A and C), effects that -at the chosen dose level and time point of analysis-occurred irrespective of SKH-1 *Nrf2* genotype. In contrast, systemic administration of bixin suppressed UV-induced epidermal thickening and apoptosis, a photoprotective effect confined to *Nrf2*$^{+/+}$ mice.

Bixin attenuates solar UV-induced epidermal oxidative DNA damage and inflammatory responses in Nrf2$^{+/+}$ but not in Nrf2$^{-/-}$ mice

Next, IHC analysis of cutaneous 8-hydroxy-2'-deoxyguanosine (8-oxo-dG), a hallmark of oxidative genomic damage in response to environmental electrophilic insult, revealed that UV-exposure equally enhanced 8-oxo-dG staining in both *Nrf2*$^{+/+}$ and *Nrf2*$^{-/-}$ mice, an effect suppressed by bixin administration (Fig. 4A). This photoprotective effect occurred in *Nrf2*$^{+/+}$ but not *Nrf2*$^{-/-}$ mice suggesting that bixin-based antioxidant photoprotection is strictly NRF2-dependent. In contrast, cyclobutane pyrimidine dimer (CPD)-lesions, a molecular hallmark of UVB-induced DNA damage that occurs independent of oxidative pathways, was not antagonized by bixin treatment and was equally pronounced in UV-exposed *Nrf2*$^{+/+}$ and *Nrf2*$^{-/-}$ mouse skin (Fig. 4A). Consistent with NRF2-dependent suppression of UV-induced epidermal thickening (Fig. 4A-B), we also observed the suppression of UV-elicited keratinocyte hyperproliferation in bixin-treated *Nrf2*$^{+/+}$ mice [as indicated by Ki67 IHC analysis (Fig. 5A)].

Next, bixin-modulation of UV-induced cutaneous inflammation was examined. IHC analysis revealed that UV-induced epidermal expression of the inflammatory NF-κB target gene *MMP9* (matrix metallopeptidase 9; gelatinase B), observable equally in *Nrf2*$^{+/+}$ and *Nrf2*$^{-/-}$ mice, was significantly antagonized by systemic delivery of bixin in *Nrf2*$^{+/+}$ mice only (Fig. 5B). Furthermore, UV-activation of the NF-κB pathway was evident from upregulated p65 phosphorylation (p-p65) detected in both *Nrf2*$^{+/+}$ and *Nrf2*$^{-/-}$ mice (Fig. 5C-D). Systemic administration of bixin decreased UV-induced p-p65 accumulation in the skin of *Nrf2*$^{+/+}$ mice, whereas bixin treatment displayed minimal effects in *Nrf2*$^{-/-}$ mice, observations consistent with prior reports on Nrf2-dependent attenuation of NF-κB [49].

In order to substantiate the bixin-elicited attenuation of UV-induced activation of the cutaneous NF-κB pathway, modulation of NF-κB target gene expression (*IL6*, *TNF*a, *MMP9*) was monitored at the mRNA level (Fig. 5E). As expected, UV-exposure upregulated cutaneous mRNA levels of NF-κB target genes in both *Nrf2*$^{+/+}$ and *Nrf2*$^{-/-}$ mice, an observation consistent with analogous published experiments examining UV-induced upregulation of IL-6, IL-1β, and COX-2 expression in *Nrf2*$^{+/+}$ and *Nrf2*$^{-/-}$ SKH-1 mice [9, 22, 49], whereas bixin-attenuation of inflammatory gene expression was observed only in *Nrf2*$^{+/+}$ mice.

DISCUSSION

Recently, the photochemopreventive effects of constitutive genetic activation of NRF2 have been described in a murine photocarcinogenesis model [22], and pharmacological activation of NRF2 has been envisioned as a novel molecular strategy for cutaneous photoprotection [9, 13-15, 19, 21, 24]. Here we have explored the specific molecular mechanism underlying carotenoid-based systemic skin photoprotection in SKH-1 mice, providing experimental evidence that systemic protection against UV-induced skin damage conferred by the dietary apocarotinoid and FDA-approved food additive bixin is NRF2 dependent.

First, we demonstrated that bixin is a canonical KEAP1-C151-dependent activator of the NRF2-orchestrated cytoprotective response in cultured human skin keratinocytes (Figs. 1-2).

Consistent with upregulation of the NRF2-controlled intracellular antioxidant response, including genes involved in glutathione biosynthesis and function (*SLC7A11*, *GCLC*, *GPX2*, *GSTZ1*, *GPX3)*, total glutathione levels were elevated significantly in human keratinocytes exposed to bixin. It has been demonstrated earlier that NRF2 establishes a glutathione-mediated gradient of UVB-cytoprotection in the epidermis, and upregulation of cellular glutathione levels has been identified as a mechanistic determinant of NRF2-dependent photoprotection [20, 24].

Next, we performed experiments demonstrating that systemic administration of bixin by intraperitoneal injection activates cutaneous NRF2 and NRF2 target gene (*AKR1C1*, *GCLM*) expression (Fig. 3). It was observed that bixin administration caused pronounced photoprotection against acute solar UV exposure, suppressing hyperproliferative skin thickening, apoptotic cell death, and oxidative DNA damage (Fig. 4). In addition, systemic intervention using bixin was able to suppress UV-induced inflammatory responses detectable at the mRNA (*IL6*, *MMP9*, *TNF*α) and protein (Ki67, MMP9, p-p65) levels (Fig. 5), data that are consistent with the established attenuation of NFκB-controlled signaling by NRF2 upregulation [9, 49]. Importantly, it was observed that bixin-induced photoprotective effects were confined to $Nrf2^{+/+}$ mice, since no photoprotective effects of bixin were detectable in $Nrf2^{-/-}$ mice. These observations are consistent with earlier reports documenting the suppression of UVB-induced acute inflammation and sunburn by topical administration of NRF2 inducers in $Nrf2^{+/+}$ mice [9, 22, 49]. HPLC-based examination of bixin plasma levels confirmed the close similarity of C_{max} and AUC between $Nrf2^{+/+}$ versus $Nrf2^{-/-}$ mice, indicating that differential photoprotective effects could not be attributed to genotype-specific differences in bixin pharmacokinetic profiles (Fig. S2; Supplementary Material). It is important to note that recent genetic evidence indicates that constitutive and persistent upregulation of NRF2 (irresponsive to KEAP1-mediated degradation) causes skin pathologies and impaired barrier function [25, 50, 51], whereas moderate upregulation of NRF2 activity through genetic attenuation of Keap1 expression displays potent photochemopreventive activity in a murine skin photocarcinogenesis model [22]. It should also be mentioned that Nrf2-activating mutations have been identified in cutaneous squamous cell carcinomas [50]. It therefore seems prudent to further explore the potential utility of topical or systemic pharmacological NRF2 activators used as stand alone or combinatorial photoprotectants of human skin in more detail [7, 11].

The concept of cutaneous photoprotection achieved by systemic administration of specific small molecule phytochemicals including carotenoids has been the subject of considerable research interest in the past [4, 27-29, 52-54]. However, no prior research has explored the NRF2-dependence of carotenoid-based systemic photoprotection as presented in this study. It remains to be seen if NRF2-dependence of antioxidant tissue protection achieved by systemic administration of the apocarotenoid bixin, a food additive devoid of provitamin A activity, also applies to other carotenoids that display photoprotective activity [4, 27-30].

Remarkably, bixin is now one of the most consumed food colorants in the world distinguished by a long record of dietary and ethnopharmacological use [33, 34]. In prior studies, bixin has demonstrated antigenotoxic and antioxidant cytoprotective activities, and systemic availability of oral bixin and its demethylated metabolite norbixin has been

documented in rodent studies and healthy human subjects [35, 36, 55, 56]. Importantly, acceptable daily intake (ADI) over a lifetime without an appreciable health risk (http://apps.who.int/food-additives-contaminants-jecfa-database/search.aspx) surpasses that of any other carotenoid approved as a food additive [ADI (bixin): 12 mg/kg body weight/day] [57]. Based on safety record, systemic availability, and our experimental evidence demonstrating NRF2-dependent skin photoprotection by systemic administration of bixin in a murine UV exposure model, our future preclinical and clinical research activities will examine efficacy of bixin-based dietary activation of cutaneous NRF2 as a novel strategy for human skin photoprotection.

Supplementary Material

Refer to Web version on PubMed Central for supplementary material.

ACKNOWLEDGEMENTS

Supported in part by grants from the National Institutes of Health [2R01ES015010, R01CA154377, R03CA167580, R21CA166926, CA023074, ES007091, ES006694].

Abbreviations

As	sodium arsenite
ARE	antioxidant response element
GCLM	glutamate-cysteine ligase, modifier subunit
KEAP1	Kelch-like ECH-associated protein 1
NRF2	nuclear factor-E2-related factor 2
8-oxo-dG	8-hydroxy-2’-deoxyguanosine
SF	sulforaphane, UVA, ultraviolet A
UVB	ultraviolet B

References

[1]. Chen H, Weng QY, Fisher DE. UV signaling pathways within the skin. J. Invest. Dermatol. 2014; 134:2080–2085. [PubMed: 24759085]

[2]. Natarajan VT, Ganju P, Ramkumar A, Grover R, Gokhale RS. Multifaceted pathways protect human skin from UV radiation. Nat. Chem. Biol. 2014; 10:542–551. [PubMed: 24937072]

[3]. Brash DE. UV signature mutations. Photochem. Photobiol. 2015; 91:15–26. [PubMed: 25354245]

[4]. Gonzalez S, Astner S, An W, Goukassian D, Pathak MA. Dietary lutein/zeaxanthin decreases ultraviolet B-induced epidermal hyperproliferation and acute inflammation in hairless mice. J. Invest. Dermatol. 2003; 121:399–405. [PubMed: 12880433]

[5]. Wondrak GT, Jacobson MK, Jacobson EL. Endogenous UVA-photosensitizers: mediators of skin photodamage and novel targets for skin photoprotection. Photochem. Photobiol. Sci. 2006; 5:215–237. [PubMed: 16465308]

[6]. Nichols JA, Katiyar SK. Skin photoprotection by natural polyphenols: anti-inflammatory, antioxidant and DNA repair mechanisms. Arch. Dermatol. Res. 2010; 302:71–83. [PubMed: 19898857]

[7]. Wondrak, GT. Sunscreen-Based Skin Protection Against Solar Insult: Molecular Mechanisms and Opportunities. In: Alberts, D., editor. Fundamentals of Cancer Prevention. Springer Science & Business Media; 2014. p. 301-320.

[8]. Suzuki T, Motohashi H, Yamamoto M. Toward clinical application of the Keap1-Nrf2 pathway. Trends Pharmacol. Sci. 2013; 34:340–346. [PubMed: 23664668]

[9]. Saw CL, Huang MT, Liu Y, Khor TO, Conney AH, Kong AN. Impact of Nrf2 on UVB-induced skin inflammation/photoprotection and photoprotective effect of sulforaphane. Mol. Carcinog. 2011; 50:479–486. [PubMed: 21557329]

[10]. Ma Q. Role of Nrf2 in oxidative stress and toxicity. Annu. Rev. Pharmacol. Toxicol. 2013; 53:401–426. [PubMed: 23294312]

[11]. Schafer M, Werner S. Nrf2-A regulator of keratinocyte redox signaling. Free Radic. Biol. Med. Apr 23.2015 [Epub ahead of print].

[12]. Hirota A, Kawachi Y, Itoh K, Nakamura Y, Xu X, Banno T, Takahashi T, Yamamoto M, Otsuka F. Ultraviolet A irradiation induces NF-E2-related factor 2 activation in dermal fibroblasts: protective role in UVA-induced apoptosis. J. Invest. Dermatol. 2005; 124:825–832. [PubMed: 15816842]

[13]. Dinkova-Kostova AT, Jenkins SN, Fahey JW, Ye L, Wehage SL, Liby KT, Stephenson KK, Wade KL, Talalay P. Protection against UV-light-induced skin carcinogenesis in SKH-1 high-risk mice by sulforaphane-containing broccoli sprout extracts. Cancer Lett. 2006; 240:243–252. [PubMed: 16271437]

[14]. Wondrak GT, Cabello CM, Villeneuve NF, Zhang S, Ley S, Li Y, Sun Z, Zhang DD. Cinnamoyl-based Nrf2-activators targeting human skin cell photo-oxidative stress. Free Radic. Biol. Med. 2008; 45:385–395. [PubMed: 18482591]

[15]. Benedict AL, Knatko EV, Dinkova-Kostova AT. The indirect antioxidant sulforaphane protects against thiopurine-mediated photooxidative stress. Carcinogenesis. 2012; 33:2457–2466. [PubMed: 22983983]

[16]. Gruber F, Mayer H, Lengauer B, Mlitz V, Sanders JM, Kadl A, Bilban M, de Martin R, Wagner O, Kensler TW, Yamamoto M, Leitinger N, Tschachler E. NF-E2-related factor 2 regulates the stress response to UVA-1-oxidized phospholipids in skin cells. FASEB J. 2010; 24:39–48. [PubMed: 19720622]

[17]. Tian FF, Zhang FF, Lai XD, Wang LJ, Yang L, Wang X, Singh G, Zhong JL. Nrf2-mediated protection against UVA radiation in human skin keratinocytes. Biosci. Trends. 2011; 5:23–29. [PubMed: 21422597]

[18]. Hirota A, Kawachi Y, Yamamoto M, Koga T, Hamada K, Otsuka F. Acceleration of UVB-induced photoageing in nrf2 gene-deficient mice. Exp. Dermatol. 2011; 20:664–668. [PubMed: 21569103]

[19]. Kalra S, Knatko EV, Zhang Y, Honda T, Yamamoto M, Dinkova-Kostova AT. Highly potent activation of Nrf2 by topical tricyclic bis(cyano enone): implications for protection against UV radiation during thiopurine therapy. Cancer Prev. Res. (Phila). 2012; 5:973–981. [PubMed: 22659146]

[20]. Schafer M, Dutsch S, auf dem Keller U, Navid F, Schwarz A, Johnson DA, Johnson JA, Werner S. Nrf2 establishes a glutathione-mediated gradient of UVB cytoprotection in the epidermis. Genes Dev. 2010; 24:1045–1058. [PubMed: 20478997]

[21]. Tao S, Justiniano R, Zhang DD, Wondrak GT. The Nrf2-inducers tanshinone I and dihydrotanshinone protect human skin cells and reconstructed human skin against solar simulated UV. Redox Biol. 2013; 1:532–541. [PubMed: 24273736]

[22]. Knatko EV, Ibbotson SH, Zhang Y, Higgins M, Fahey JW, Talalay P, Dawa R, Ferguson J, Huang JT, Clarke R, Zheng S, Saito A, Kalra S, Benedict AL, Honda T, Proby CM, Dinkova-Kostova AT. Nrf2 activation protects against solar-simulated ultraviolet radiation in mice and humans. Cancer Prev. Res. (Phila). 2015; 8:475–86. [PubMed: 25804610]

[23]. Chun KS, Kundu J, Kundu JK, Surh YJ. Targeting Nrf2-Keap1 signaling for chemoprevention of skin carcinogenesis with bioactive phytochemicals. Toxicol. Lett. 2014; 229:73–84. [PubMed: 24875534]

[24]. Lieder F, Reisen F, Geppert T, Sollberger G, Beer HD, auf dem Keller U, Schafer M, Detmar M, Schneider G, Werner S. Identification of UV-protective activators of nuclear factor erythroid-derived 2-related factor 2 (Nrf2) by combining a chemical library screen with computer-based virtual screening. J Biol. Chem. 2012; 287:33001–33013. [PubMed: 22851183]

[25]. Schafer M, Farwanah H, Willrodt AH, Huebner AJ, Sandhoff K, Roop D, Hohl D, Bloch W, Werner S. Nrf2 links epidermal barrier function with antioxidant defense. EMBO Mol. Med. 2012; 4:364–379. [PubMed: 22383093]

[26]. Dinkova-Kostova AT, Fahey JW, Benedict AL, Jenkins SN, Ye L, Wehage SL, Talalay P. Dietary glucoraphanin-rich broccoli sprout extracts protect against UV radiation-induced skin carcinogenesis in SKH-1 hairless mice. Photochem. Photobiol. Sci. 2010; 9:597–600. [PubMed: 20354656]

[27]. Sies H, Stahl W. Nutritional Protection Against Skin Damage From Sunlight. Annu. Rev. Nutr. 2004; 24:173–200. [PubMed: 15189118]

[28]. Astner S, Wu A, Chen J, Philips N, Rius-Diaz F, Parrado C, Mihm MC, Goukassian DA, Pathak MA, Gonzalez S. Dietary lutein/zeaxanthin partially reduces photoaging and photocarcinogenesis in chronically UVB-irradiated Skh-1 hairless mice. Skin Pharmacol. Physiol. 2007; 20:283–291. [PubMed: 17717424]

[29]. Stahl W, Sies H. beta-Carotene and other carotenoids in protection from sunlight. Am. J. Clin. Nutr. 2012; 96:1179S–1184S. [PubMed: 23053552]

[30]. Fernandez-Garcia E. Skin protection against UV light by dietary antioxidants. Food Funct. 2014; 5:1994–2003. [PubMed: 24964816]

[31]. Di Mascio P, Kaiser S, Sies H. Lycopene as the most efficient biological carotenoid singlet oxygen quencher. Arch. Biochem. Biophys. 1989; 274:532–538. [PubMed: 2802626]

[32]. Di Mascio P, Devasagayam TP, Kaiser S, Sies H. Carotenoids, tocopherols and thiols as biological singlet molecular oxygen quenchers. Biochem. Soc. Trans. 1990; 18:1054–1056. [PubMed: 2088803]

[33]. Ulbricht C, Windsor RC, Brigham A, Bryan JK, Conquer J, Costa D, Giese N, Guilford J, Higdon ER, Holmes K, Isaac R, Jingst S, Kats J, Peery L, Rusie E, Savinainen A, Schoen T, Stock T, Tanguay-Colucci S, Weissner W. An evidence-based systematic review of annatto (Bixa orellana L.) by the Natural Standard Research Collaboration. J. Diet Suppl. 2012; 9:57–77. [PubMed: 22432803]

[34]. Stohs SJ. Safety and efficacy of Bixa orellana (achiote, annatto) leaf extracts. Phytother. Res. 2014; 28:956–960. [PubMed: 24357022]

[35]. Levy LW, Regalado E, Navarrete S, Watkins RH. Bixin and norbixin in human plasma: determination and study of the absorption of a single dose of Annatto food color. Analyst. 1997; 122:977–980. [PubMed: 9374027]

[36]. Junior AC, Asad LM, Oliveira EB, Kovary K, Asad NR, Felzenszwalb I. Antigenotoxic and antimutagenic potential of an annatto pigment (norbixin) against oxidative stress. Genet. Mol. Res. 2005; 4:94–99. [PubMed: 15841440]

[37]. World Health, O. Evaluation of certain food additives and contaminants. World Health Organ. Tech. Rep. Ser. 2013:1–75. back cover.

[38]. Wondrak GT, Roberts MJ, Cervantes-Laurean D, Jacobson MK, Jacobson EL. Proteins of the Extracellular Matrix Are Sensitizers of Photo-oxidative Stress in Human Skin Cells. J. Invest. Dermatol. 2003; 121:578–586. [PubMed: 12925218]

[39]. Williams JD, Bermudez Y, Park SL, Stratton SP, Uchida K, Hurst CA, Wondrak GT. Malondialdehyde-derived epitopes in human skin result from acute exposure to solar UV and occur in nonmelanoma skin cancer tissue. J. Photochem. Photobiol. B. 2014; 132:56–65. [PubMed: 24584085]

[40]. Park SL, Justiniano R, Williams JD, Cabello CM, Qiao S, Wondrak GT. The Tryptophan-Derived Endogenous Aryl Hydrocarbon Receptor Ligand 6-Formylindolo[3,2-b]Carbazole Is a Nanomolar UVA Photosensitizer in Epidermal Keratinocytes. J. Invest. Dermatol. 2015; 135:1649–1658. [PubMed: 25431849]

[41]. Lamore SD, Qiao S, Horn D, Wondrak GT. Proteomic identification of cathepsin B and nucleophosmin as novel UVA-targets in human skin fibroblasts. Photochem. Photobiol. 2010; 86:1307–1317. [PubMed: 20946361]

[42]. Qiao S, Tao S, Rojo de la Vega M, Park SL, Vonderfecht AA, Jacobs SL, Zhang DD, Wondrak GT. The antimalarial amodiaquine causes autophagic-lysosomal and proliferative blockade sensitizing human melanoma cells to starvation- and chemotherapy-induced cell death. Autophagy. 2013; 9:2087–2102. [PubMed: 24113242]

[43]. Tao S, Zheng Y, Lau A, Jaramillo MC, Chau BT, Lantz RC, Wong PK, Wondrak GT, Zhang DD. Tanshinone I Activates the Nrf2-Dependent Antioxidant Response and Protects Against As(III)-Induced Lung Inflammation In Vitro and In Vivo. Antioxid. Redox Signal. 2013; 19:1647–61. [PubMed: 23394605]

[44]. Wondrak GT, Jacobson MK, Jacobson EL. Identification of quenchers of photoexcited states as novel agents for skin photoprotection. J. Pharmacol. Exp. Ther. 2005; 312:482–491. [PubMed: 15475591]

[45]. Moi P, Chan K, Asunis I, Cao A, Kan YW. Isolation of NF-E2-related factor 2 (Nrf2), a NF-E2-like basic leucine zipper transcriptional activator that binds to the tandem NF-E2/AP1 repeat of the beta-globin locus control region. Proc. Natl. Acad. Sci. U S A. 1994; 91:9926–9930. [PubMed: 7937919]

[46]. Monticone M, Taherian R, Stigliani S, Carra E, Monteghirfo S, Longo L, Daga A, Dono M, Zupo S, Giaretti W, Castagnola P. NAC, tiron and trolox impair survival of cell cultures containing glioblastoma tumorigenic initiating cells by inhibition of cell cycle progression. PLoS One. 2014; 9:e90085. [PubMed: 24587218]

[47]. Zhang DD, Hannink M. Distinct cysteine residues in Keap1 are required for Keap1-dependent ubiquitination of Nrf2 and for stabilization of Nrf2 by chemopreventive agents and oxidative stress. Mol. Cell. Biol. 2003; 23:8137–8151. [PubMed: 14585973]

[48]. Lau A, Zheng Y, Tao S, Wang H, Whitman SA, White E, Zhang DD. Arsenic Inhibits Autophagic Flux, Activating the Nrf2-Keap1 Pathway in a p62-Dependent Manner. Mol. Cell. Biol. 2013; 33:2436–2446. [PubMed: 23589329]

[49]. Li W, Khor TO, Xu C, Shen G, Jeong WS, Yu S, Kong AN. Activation of Nrf2-antioxidant signaling attenuates NFkappaB-inflammatory response and elicits apoptosis. Biochem. Pharmacol. 2008; 76:1485–1489. [PubMed: 18694732]

[50]. Kim YR, Oh JE, Kim MS, Kang MR, Park SW, Han JY, Eom HS, Yoo NJ, Lee SH. Oncogenic NRF2 mutations in squamous cell carcinomas of oesophagus and skin. J. Pathol. 2010; 220:446–451. [PubMed: 19967722]

[51]. Schafer M, Willrodt AH, Kurinna S, Link AS, Farwanah H, Geusau A, Gruber F, Sorg O, Huebner AJ, Roop DR, Sandhoff K, Saurat JH, Tschachler E, Schneider MR, Langbein L, Bloch W, Beer HD, Werner S. Activation of Nrf2 in keratinocytes causes chloracne (MADISH)-like skin disease in mice. EMBO Mol. Med. 2014; 6:442–457. [PubMed: 24503019]

[52]. Vayalil PK, Mittal A, Hara Y, Elmets CA, Katiyar SK. Green tea polyphenols prevent ultraviolet light-induced oxidative damage and matrix metalloproteinases expression in mouse skin. J. Invest. Dermatol. 2004; 122:1480–1487. [PubMed: 15175040]

[53]. Gonzalez S, Gilaberte Y, Philips N. Mechanistic insights in the use of a Polypodium leucotomos extract as an oral and topical photoprotective agent. Photochem. Photobiol. Sci. 2010; 9:559–563. [PubMed: 20354651]

[54]. Chen AC, Damian DL, Halliday GM. Oral and systemic photoprotection. Photodermatol. Photoimmunol. Photomed. 2014; 30:102–111. [PubMed: 24313740]

[55]. Somacal S, Figueiredo CG, Quatrin A, Ruviaro AR, Conte L, Augusti PR, Roehrs M, Denardin IT, Kasten J, da Veiga ML, Duarte MM, Emanuelli T. The antiatherogenic effect of bixin in hypercholesterolemic rabbits is associated to the improvement of lipid profile and to its antioxidant and anti-inflammatory effects. Mol. Cell. Biochem. 2015; 403:243–253. [PubMed: 25702177]

[56]. Roehrs M, Figueiredo CG, Zanchi MM, Bochi GV, Moresco RN, Quatrin A, Somacal S, Conte L, Emanuelli T. Bixin and norbixin have opposite effects on glycemia, lipidemia, and oxidative stress in streptozotocin-induced diabetic rats. Int. J. Endocrinol. 2014; 2014:839095. [PubMed: 24624139]

[57]. WHO. Evaluation of certain food additives and contaminants. Thirty-fifth report of the Joint FAO/WHO Expert Committee on Food Additives. Tech. Rep. Ser. 1990; 789:1–48.

HIGHLIGHTS

- The dietary apocarotenoid bixin activates NRF2 through Cys-151 in KEAP1.
- Bixin orchestrates a broad cytoprotective response in cultured human keratinocytes.
- Systemic administration of bixin activates cutaneous NRF2 in SKH-1 mice.
- Systemic bixin attenuates acute photodamage in $Nrf2^{+/+}$ but not in $Nrf2^{-/-}$ mice.

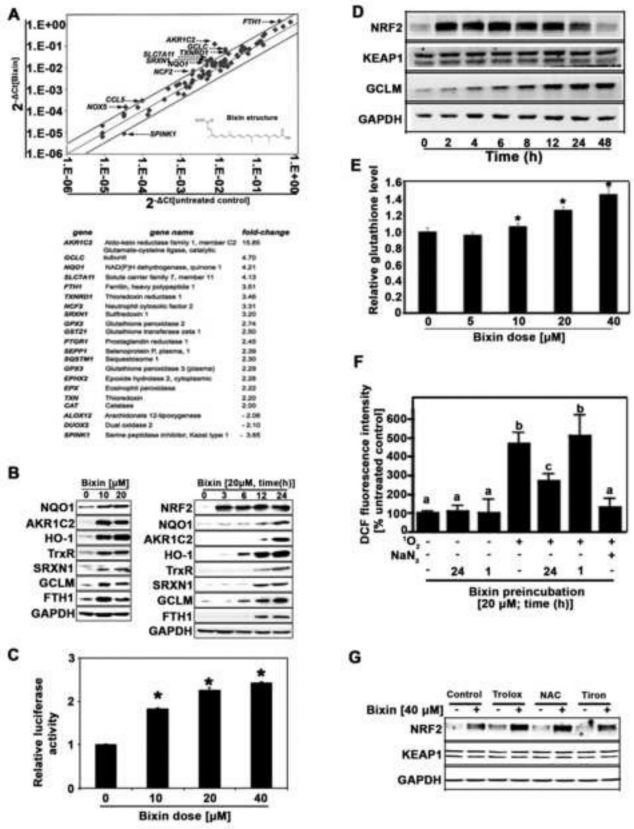

Figure 1. Bixin upregulates NRF2 signaling and antioxidant defenses in epidermal keratinocytes

(A) For Oxidative Stress RT^2 Profiler^{TM} PCR Expression Array analysis, HEKs were exposed to bixin (20 μM, 24 h) followed by gene expression analysis; upper panel: scatter blot depiction of bixin-induced gene expression (versus untreated); cut-off lines: threefold up- or down-regulation; the insert shows the chemical structure of bixin; bottom panel: numerical expression changes [n=3, mean ± SD; ($p<0.05$)]. (B) Bixin (0-20 μM, 0-24 h) increased the protein levels of NRF2 and its target genes as assessed by immunoblot analysis; left panel: dose-response, right panel: time course. (C) HaCaT keratinocytes cotransfected with NQO1-ARE firefly luciferase and *Renilla* luciferase reporters were treated with bixin (0-40 μM) for 16 h. Dual luciferase activities were measured; data are expressed as means ± SD (*$p<0.05$, ctrl. *vs.* bixin treated groups). (D) HaCaT keratinocytes were treated with bixin (20 μM; 0-48 h exposure time), and cell lysates were subjected to immunoblot analysis. (E) HaCaT keratinocytes were treated with bixin (0-40 μM, 24 h), and total cellular glutathione was determined [n=3; means ± SD (*$p<0.05$, ctrl. *vs.* bixin groups]. (F) HaCaT keratinocytes were exposed to bixin (20 μM; 1 and 24 h exposure time) followed by dye sensitization (generating $^1O_2$) and subsequent loading with 2',7'-dichlorodihydrofluorescein diacetate (DCFH-DA)]. Intracellular oxidative stress was then assessed by flow cytometric determination of DCF fluorescence intensity [means ± SD, n=3; means without a common letter differ ($p < 0.05$)]. (G) HaCaT keratinocytes were exposed to various anti-oxidants [1 h pretreatment: trolox (1 mM), tiron (500 μM), N-acetyl-L-cysteine (NAC; 10 mM)] followed by addition of bixin (40 μM; 4 h) and NRF2/KEAP1 immunoblot analysis.

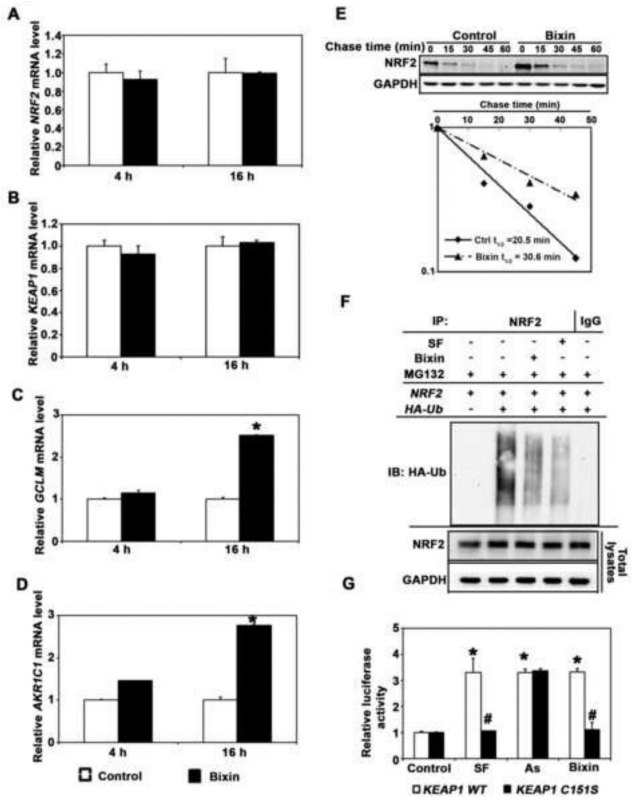

Figure 2. Bixin induces KEAP1-C151-dependent NRF2 upregulation and increases

Nrf2 protein half-life ($t_{1/2}$) in human keratinocytes. (A-D) HaCaT cells were either left untreated (control; empty bar) or treated with bixin (40 μM, filled bar; 4 h and 16 h), and mRNA was extracted. Relative mRNA levels [*NRF2* (A), *KEAP1* (B), *GCLM* (C), *AKR1C1* (D)] as determined by quantitative real-time RT-PCR [means ± SD (*p<0.05, control *vs.* bixin treated group)]. (E) HaCaT cells were either left untreated or treated with bixin (40 μM, 4h). Cycloheximide (CHX, 50 μM) was added and cells were lysed at the indicated time points followed by immunoblot analysis using NRF2 and GAPDH antibodies. Band intensities were quantified and plotted against the time after CHX treatment to obtain half-life ($t_{1/2}$) values. (F) HaCaT cells were cotransfected with plasmids encoding the indicated proteins; 24 h later the cells were then left untreated or treated with either SF (5 μM) or bixin (40 μM) along with MG132 (10 μM) for 4 h. Anti-NRF2 immunoprecipitates were analyzed by immunoblotting with anti-HA antibody detecting ubiquitin-conjugated NRF2. (G) HaCaT cells cotransfected with the plasmids expressing either wild type *KEAP1* (*KEAP1-WT*) or C151 mutated *KEAP1* (*KEAP1-C151S*) along with *NQO1-ARE* firefly luciferase and *Renilla* luciferase reporters were left untreated or treated with the indicated compounds (16 h). Dual luciferase activities were measured; data are expressed as means ± SD (*p<0.05, Control *vs.* compound treated groups; $^{\#}p$<0.05, *KEAP1-WT vs. KEAP1-C151S* group.)

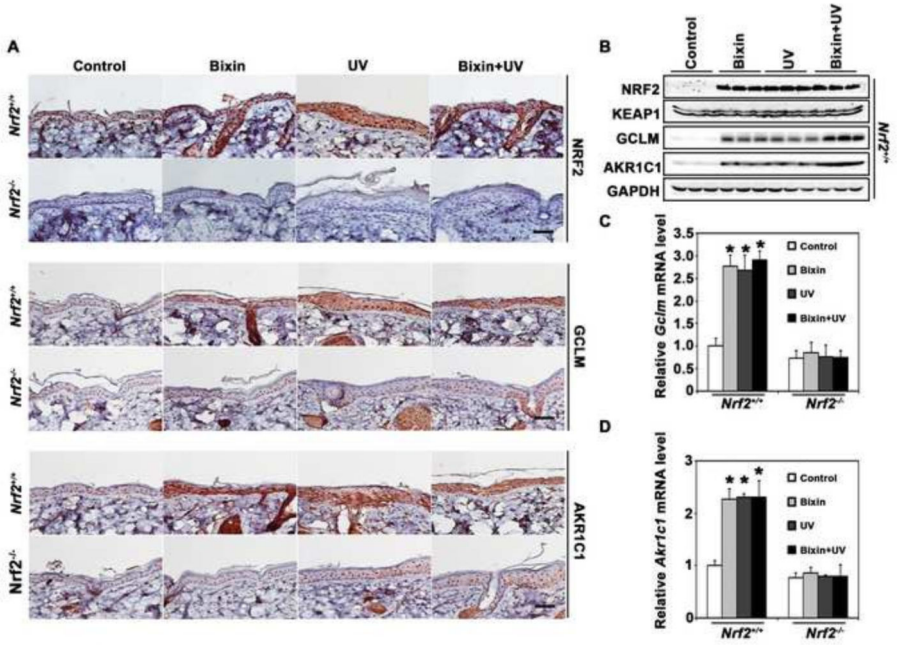

Figure 3. Systemic administration of bixin activates cutaneous NRF2 and NRF2 targets

Mice (*Nrf2*$^{+/+}$ and *Nrf2*$^{-/-}$ mice; n = 6 per group) received bixin treatment (200 mg/kg; i.p.) or carrier control (corn oil), followed by solar UV (UVB 240 mJ/cm^2) or mock exposure performed 48 h after bixin administration. (A) After UV exposure (24 h), IHC analysis (NRF2, GCLM, AKR1C1) was performed using skin tissue sections; representative tissue from each group is shown (scale bar: 100 μm). (B) Skin tissue lysates from *Nrf2*$^{+/+}$ mice were subjected to immunoblot analyses with anti-NRF2, KEAP1, AKR1C1, GCLM, and GAPDH antibodies (n=3, each lane represents an individual mouse). (C-D) Skin prepared from mice as specified in (A) was processed for determination of mRNA levels [*Gclm* (C) and *Akr1c1* (D)] using quantitative RT-PCR; means ± SD (*p<0.05, control *vs.* treatment groups).

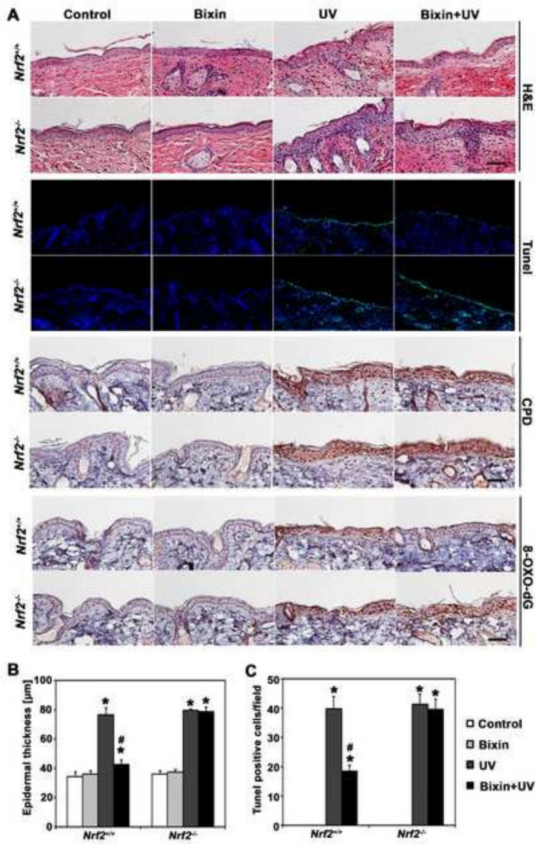

Figure 4. Systemic administration of bixin suppresses UV-induced epidermal thickening, apoptosis, and oxidative DNA damage in *Nrf2*$^{+/+}$ mice but not *Nrf2*$^{-/-}$ mice

Mice (*Nrf2*$^{+/+}$ and *Nrf2*$^{-/-}$ mice; n = 6 per group) received bixin treatment (200 mg/kg; i.p.) or carrier control (corn oil), followed by solar UV (UVB 240 mJ/cm^2) or mock exposure performed 48 h after bixin. (A) After irradiation (24 h), H&E staining and *in situ* TUNEL analysis visualizing epidermal apoptotic cells were performed [n = 6; representative tissue from each group is shown (scale bar: 100 μm)]. In addition, 8-oxo-dG- and CPD-lesions were visualized by IHC; representative tissue from each group is shown. (B) Epidermal thickness in H&E-stained sections was measured as the distance between the top of the basement membrane and the bottom of the stratum corneum at five randomly selected fields from each mouse specimen. (C) Quantification of TUNEL-positive cells (green fluorescent nuclei) in five random fields per section; 200 × magnification; [means ± SD (*p<0.05, control *vs.* treatment groups; $^{\#}p$<0.05, UV *vs.* bixin+UV groups)].

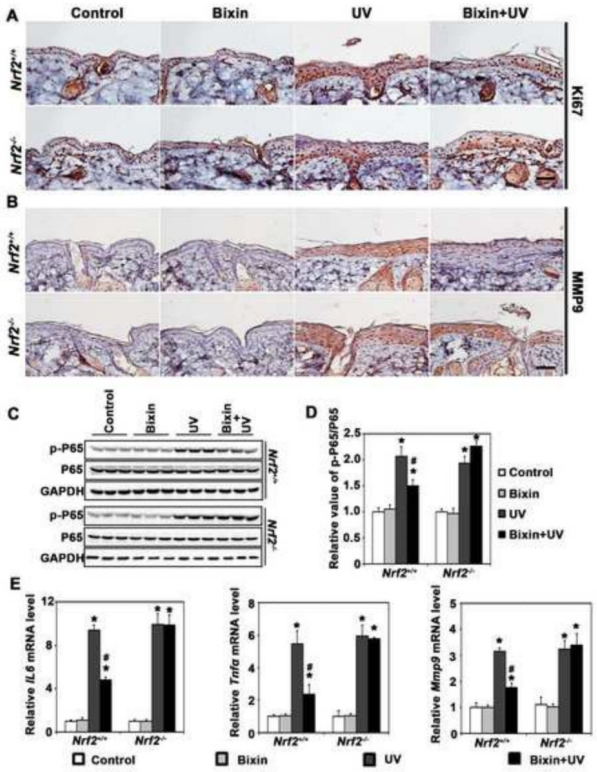

Figure 5. Systemic administration of bixin attenuates UV-induced cutaneous hyperproliferation and inflammation in *Nrf2*$^{+/+}$ mice but not *Nrf2*$^{-/-}$ mice

Mice were treated as detailed in Figs. 3 and 4 followed by IHC analysis for (A) Ki67 and (B) MMP9 (scale bar: 100 μm). (C-D) Skin tissue lysates from bixin/UV-exposed *Nrf2*$^{+/+}$ and *Nrf2*$^{-/-}$ mice were also subjected to immunoblot analyses with anti-p-p65, p65, and GADPH antibodies followed by quantification using densitometry (D). (E) mRNA levels of *IL6*, *TNF*a and *MMP9* were determined using quantitative RT-PCR. Results are expressed as means ± SD (*p<0.05, control *vs.* treatment groups; $^{\#}p$<0.05, UV *vs.* bixin+UV groups).